Development of ADI-FDTD Methods with Dispersion-Relation-Preserving Features

T. T. Zygiridis[1], **N. V. Kantartzis**[2], **and T. D. Tsiboukis**[2]

[1]Department of Informatics & Telecommunications Engineering, University of Western Macedonia, Greece
[2]Department of Electrical & Computer Engineering, Aristotle University of Thessaloniki, Greece

Abstract— We present two methodologies that improve the performance of the alternating-direction-implicit (ADI) finite-difference time-domain (FDTD) scheme. The first one exploits optimized spatial operators and implements an artificial-anisotropy approach, so that errors around a central frequency are minimized. According to the second scheme, a matching-terms procedure is applied to the dispersion relation, so that approximations that improve space-time errors in a wideband fashion are obtained. The successful implementation of these principles is validated theoretically, while numerical tests reveal their advantageous properties in practical simulations.

1. INTRODUCTION

Being free of time-step limitations, unconditionally-stable computational methods are appropriate for densely-sampled discrete models, despite exhibiting higher complexity than more classic methodologies, such as the explicit finite-difference time-domain (FDTD) scheme [1]. Unconditional stability is a fundamental feature of specific implicit FDTD algorithms, which include the alternating-direction-implicit (ADI) method [2], the locally-one-dimensional approach [3], the Crank-Nicolson technique [4] and other split-step methodologies [5].

Our interest herein is focused on the 3D ADI-FDTD method with fourth-order spatial operators and the improvement of its accuracy, while avoiding augmentation of the computational cost. Given the significance of unconditional stability, various solutions that mitigate discretization errors have been already presented. For instance, a parameter-optimized 2D ADI-FDTD method is developed in [6], while a similar parameterization based on the (2, 4) stencil is described in [7]. The incorporation of additional terms related to the truncated ones in the implicit updates is proposed for the error-reduced ADI algorithms of [8]. In [9], the use of compact high-order finite differences that also reduce the bandwidth of the involved matrices is suggested. Anisotropic parameters are exploited in [10] as a means of controlling errors at a selected frequency, while artificial anisotropy is combined with high-order operators in [11]. More recently, correctional coefficients are introduced in [12] in the context of the one-step leapfrog ADI-FDTD scheme.

The main contribution of this paper is the development of two approaches capable of increasing the reliability of the 3D ADI-FDTD algorithm. The first scheme introduces novel spatial operators with three-cell stencils, which are designed to minimize the error of the approximate differentiation of specific test functions. The new expressions are then combined with artificial anisotropy, so that flaws are corrected around a central frequency. The second approach has a more wideband effect and relies on the numerical dispersion relation of the method. By requiring the matching of low-order terms, modified second-order spatial operators are deduced that compensate for the combined space-time errors. It is shown that both solutions improve the ADI-FDTD algorithm with standard fourth-order operators, proving that non-traditional methodologies can be exploited for the performance upgrade of unconditionally-stable schemes.

2. METHODOLOGY

The ADI-FDTD method is a perturbation of the Crank-Nicolson scheme and is commonly realized as a two-stage process with implicit update equations:

$$\left(\mathbf{I}-\frac{\Delta t}{2}\mathbf{A}\right)\mathbf{u}^{n+1/2}=\left(\mathbf{I}+\frac{\Delta t}{2}\mathbf{B}\right)\mathbf{u}^{n},\quad \left(\mathbf{I}-\frac{\Delta t}{2}\mathbf{B}\right)\mathbf{u}^{n+1}=\left(\mathbf{I}+\frac{\Delta t}{2}\mathbf{A}\right)\mathbf{u}^{n+1/2} \tag{1}$$

where $\mathbf{A}$, $\mathbf{B}$ are derivative matrices,

$$\mathbf{A} = \begin{bmatrix} \mathbf{0} & \mathbf{A}_h \\ \mathbf{A}_e & \mathbf{0} \end{bmatrix}, \quad \mathbf{A}_h = \frac{1}{\epsilon}\begin{bmatrix} 0 & 0 & D_y \\ D_z & 0 & 0 \\ 0 & D_x & 0 \end{bmatrix}, \quad \mathbf{A}_e = \frac{1}{\mu}\begin{bmatrix} 0 & D_z & 0 \\ 0 & 0 & D_x \\ D_y & 0 & 0 \end{bmatrix} \tag{2}$$

$$\mathbf{B} = \begin{bmatrix} \mathbf{0} & \mathbf{B}_h \\ \mathbf{B}_e & \mathbf{0} \end{bmatrix}, \quad \mathbf{B}_h = -\frac{1}{\epsilon}\begin{bmatrix} 0 & D_z & 0 \\ 0 & 0 & D_x \\ D_y & 0 & 0 \end{bmatrix}, \quad \mathbf{B}_e = -\frac{1}{\mu}\begin{bmatrix} 0 & 0 & D_y \\ D_z & 0 & 0 \\ 0 & D_x & 0 \end{bmatrix} \tag{3}$$

$\mathbf{I}$ is the identity matrix, and $\mathbf{u} = [E_x\, E_y\, E_z\, H_x\, H_y\, H_z]^T$ is the vector of all field components. Our goal is to modify only the derivative matrices, yet derive algorithms with lowered space-time errors. In this framework, the following operators are considered to be used in (2), (3):

$$D_u f|_i = \frac{1}{\Delta u}\left[C_1^u \left(f|_{i+\frac{1}{2}} - f|_{i-\frac{1}{2}}\right) + C_2^u \left(f|_{i+\frac{3}{2}} - f|_{i-\frac{3}{2}}\right)\right], \quad u \in \{x, y, z\} \tag{4}$$

2.1. Improvement around a Center Frequency

The first approach entails a two-step implementation. First a set of new spatial approximations, designed according to dispersion-controlling principles, is derived. Specifically, the errors pertinent to the parametric operators (4) can be estimated, when the test function $e^{-j\mathbf{k}\cdot\mathbf{r}}$ is considered. For simplicity, we examine the case of the D_z operator only. Given that it is $\frac{\partial}{\partial z} e^{-j\mathbf{k}\cdot\mathbf{r}} = -jk\cos\theta e^{-j\mathbf{k}\cdot\mathbf{r}}$, the error related to D_z can be described by the formula

$$\mathcal{E}_z = \frac{2}{\Delta u}\sum_{\ell=1}^{2} C_z^\ell \sin\left(\frac{2\ell-1}{2}k\cos\theta\Delta z\right) - k\cos\theta \tag{5}$$

To reduce the above error uniformly, the expansion of (5) in terms of spherical harmonic functions Y_ℓ^m is exploited. In essence, it is found that $\mathcal{E}_z = \mathcal{E}_z^1 Y_1^0 + \mathcal{E}_z^3 Y_3^0 + \ldots$, where

$$Y_1^0(\theta,\phi) = \sqrt{\frac{3}{4\pi}}\cos\theta, \quad Y_3^0(\theta,\phi) = \sqrt{\frac{7}{4\pi}}\left(\frac{5}{2}\cos^3\theta - \frac{3}{2}\cos\theta\right) \tag{6}$$

By canceling the lowest terms ($\mathcal{E}_z^1 = \mathcal{E}_z^3 = 0$), the unknown coefficients can be determined:

$$\begin{bmatrix} Z_1\left(\frac{\pi}{N_z}\right) & \frac{1}{9}Z_1\left(\frac{3\pi}{N_z}\right) \\ Z_2\left(\frac{\pi}{N_z}\right) & \frac{1}{81}Z_2\left(\frac{3\pi}{N_z}\right) \end{bmatrix}\begin{bmatrix} C_1^z \\ C_2^z \end{bmatrix} = \begin{bmatrix} \frac{1}{3}\left(\frac{\pi}{N_z}\right)^3 \\ 0 \end{bmatrix} \tag{7}$$

where $Z_1(x) = \sin x - x\cos x$, $Z_2(x) = x(x^2 - 15)\cos x + 3(5 - 2x^2)\sin x$, and $N_z = \lambda/\Delta z$. A similar procedure is followed for the calculation of the remaining spatial approximations.

In practice, the above-analyzed finite differences are not sufficient, since the implementation of ADI algorithms is commonly combined with time-steps larger than standard stability limits. Hence, the pertinent temporal error is the dominant one, and it cannot be handled by simply incorporating the new operators (4), (7). Since further calibration of the computational scheme is required, an improved version of the artificial anisotropy approach is also incorporated. This technique modifies the properties of the background medium, by introducing a modified substitute with diagonal anisotropy. It is based on the scheme's numerical dispersion relation, which has the form

$$\frac{\tan^2\left(\frac{\omega\Delta t}{2}\right)}{c_0^2\Delta t^2} = \frac{4c_0^2\Delta t^2\left(\frac{S_x^2 S_y^2}{\epsilon_{rx}\epsilon_{ry}\epsilon_{rz}^2} + \frac{S_y^2 S_z^2}{\epsilon_{rx}^2\epsilon_{ry}\epsilon_{rz}} + \frac{S_z^2 S_x^2}{\epsilon_{rx}\epsilon_{ry}^2\epsilon_{rz}}\right) - 16\left(\frac{S_x^2}{\epsilon_{ry}\epsilon_{rz}} + \frac{S_y^2}{\epsilon_{rx}\epsilon_{rz}} + \frac{S_z^2}{\epsilon_{rx}\epsilon_{ry}}\right)}{64 - \left(c_0^3\Delta t^3\frac{S_x S_y S_z}{\epsilon_{rx}\epsilon_{ry}\epsilon_{rz}}\right)^2} \tag{8}$$

where ϵ_{rx}, ϵ_{ry}, ϵ_{rz} denote the relative permittivities along the three axes and

$$S_u = -\frac{2j}{\Delta u}\left[C_1^u \sin\left(\tfrac{1}{2}k_u\Delta u\right) + C_2^u \sin\left(\tfrac{3}{2}k_u\Delta u\right)\right], \quad u \in \{x, y, z\} \tag{9}$$

Now, ϵ_{rx}, ϵ_{ry}, ϵ_{rz} are treated as design parameters. First, their values that guarantee zero error at three directions ($(\theta, \phi) = (0, \phi)$, $(\frac{\pi}{2}, 0)$, $(\frac{\pi}{2}, \frac{\pi}{2})$) are obtained. Then, the average error, defined as

$$AE = \frac{1}{4\pi} \int_0^{2\pi} \int_0^{\pi} \frac{\tilde{c} - c_0}{c_0} \sin\theta d\theta d\phi \tag{10}$$

is estimated, and a correction to the light speed is performed ($c_0 \leftarrow c_0(1 + AE)$), so that the re-calculation of the material parameters leads to a mean error closer to zero. This procedure is repeated until convergence is achieved. A flowchart that sketches the aforementioned implementation is given in Fig. 1(a). The influence of the material modification and the new operators on the scheme's performance is evident in Fig. 1(b), where the average value of the % error is plotted as a function of the grid density, in the case of cubic cells and $Q = 5$ ($Q = c_0\Delta t\sqrt{\Delta x^{-2} + \Delta y^{-2} + \Delta z^{-2}}$). As observed, the proposed modification enables controlling the performance of the ADI-FDTD method, by reducing errors around the selected frequencies of interest.

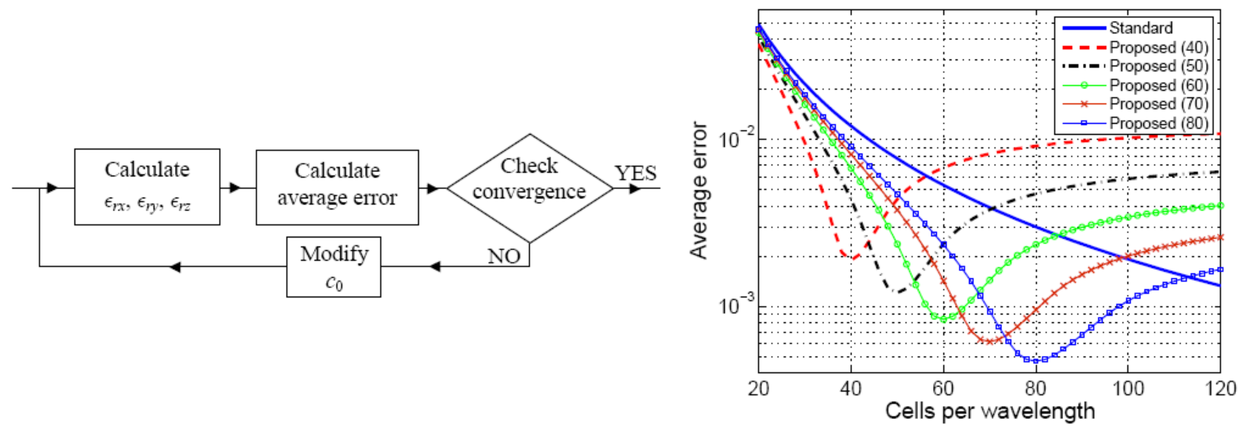

(a) (b)

Figure 1: (a) Flowchart depicting the calculation of the artificial anisotropy parameters. (b) Average error versus mesh density for the first optimization method (the point of error minimization is given in brackets).

2.2. Wideband Design Based on the Dispersion Relation

We now investigate the potential of improving the ADI-FDTD algorithm in a more wideband context. It is desirable that the modified operators should include constant, rather than frequency-dependent coefficients, since the latter are optimum only at one frequency point. To ensure that spatial and temporal errors remain balanced for all frequencies, the spatial operators are selected to be second-order accurate, by enforcing $C_1^u + 3C_2^u = 1$, $u \in \{x, y, z\}$. Additional constraints are obtained via proper manipulation of the dispersion relation. If the latter is written as $DR(\omega, \tilde{k}, \theta, \phi) = 0$, then $DR(\omega, \omega/c_0, \theta, \phi)$ can be considered to reflect discretization errors. In essence, we obtain the formula

$$\begin{aligned} DR\left(\omega, \frac{\omega}{c_0}, \theta, \phi\right) \simeq \frac{1}{6}\left(\frac{\omega}{c_0}\right)^4 (c_0\Delta t)^4 + \Bigg\{ \frac{1}{64} k_x^2 k_y^2 k_z^2 k_0^2 q^2 - \frac{1}{4}\Bigg[\left(k_x^2 k_y^2 + k_x^2 k_z^2 + k_y^2 k_z^2\right) q^2 \\ + \frac{4}{3}\left((C_1^x + 27C_2^x)\, k_x^4 + (C_1^y + 27C_2^y)\, k_y^4 {R_y}^2 + (C_1^z + 27C_2^z)\, k_z^4 {R_z}^2 \right) \Bigg] \Bigg\} \Delta x^2 \end{aligned} \tag{11}$$

where $\Delta t = q\Delta x/c_0$ and $R_u = \Delta u/\Delta x$. We should choose spatial operators that reduce the magnitude of the aforementioned expression. Since three more equations are required, a simple approach entails the selection of specific directions that correspond to the three axes, where $DR \simeq 0$ is enforced. In this way, the obtained coefficients do not exhibit any frequency dependency, and the accuracy improvement is guaranteed over all wavelengths. Specifically, we end up with:

$$C_1^u + 27C_2^u = -\frac{2q^2}{R_u^2}, \quad u \in \{x, y, z\} \tag{12}$$

Combined with the requirements for second-order accuracy, (12) yields the following coefficients:

$$C_1^u = \frac{9}{8} + \frac{q^2}{4R_u^2}, \quad C_2^u = -\frac{1}{24} - \frac{q^2}{12R_u^2}, \quad u \in \{x, y, z\} \tag{13}$$

which reduce to the values of the fourth-order operators only in the limit case of a zero time-step.

An assessment of the new operators' positive contribution is made in Figs. 2(a) and 2(b), where the error $|1 - \tilde{c}/c_0| \cdot 100\%$ is plotted in spherical coordinates (case of cubic cells with $\lambda/50$ sides, $Q = 5$). A non-trivial improvement is accomplished, as the maximum error is reduced by 5.85 times. Actually, a similar conclusion can be drawn even if the error is integrated (averaged) over all directions (reduction by 6.53 times is then observed). If the performance is examined over a range of frequencies, then one verifies the unsuitability of conventional operators, which fail to address the issue of low-order temporal accuracy. This property is evident in Fig. 3, where the average error versus mesh density is given for different time-step sizes ($Q = 5$ and $Q = 10$). From this result, it is concluded that the proposed methodology produces a more consistent discretization scheme, compared to the standard (2, 4) stencil.

3. NUMERICAL RESULTS

In the first numerical test a $4 \times 4 \times 4\,\text{cm}^3$ cavity is considered, where the (2, 1, 1) mode at 9.179 GHz is excited. The L_2 error with respect to E_x is recorded for a time period that corresponds to 1000 iterations in the case of the 90^3-cell mesh. We select $Q = 5$, i.e., a time-step five-times larger than the common stability limit. Fig. 4(a) compares the maximum L_2 values for different grids, in the case of the standard fourth-order operators and the scheme of Subsection 2.1. The depicted results

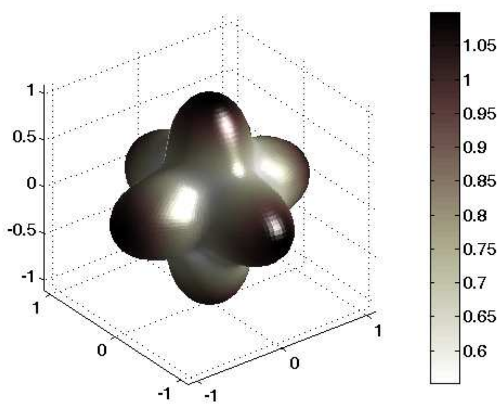

(a)

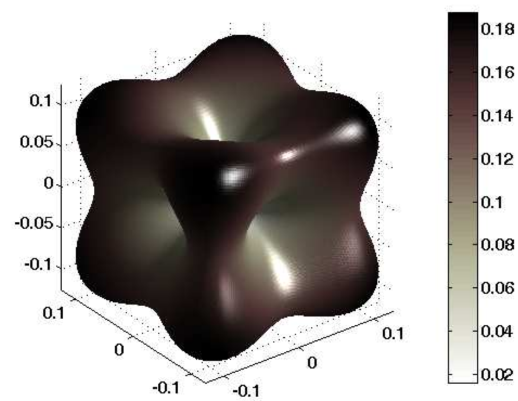

(b)

Figure 2: 3D % error in numerical velocity ($Q = 5$, $\Delta x = \lambda/50$, $R_y = R_z = 1$) in the case of (a) fourth-order operators, and (b) proposed operators (13).

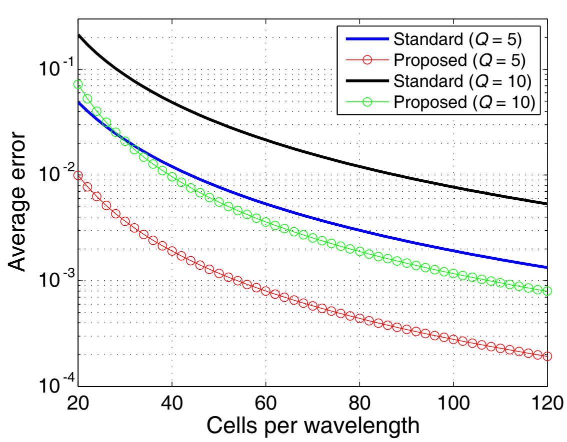

Figure 3: Average error versus discretization density for fourth-order and wideband operators ($R_y = R_z = 1$).

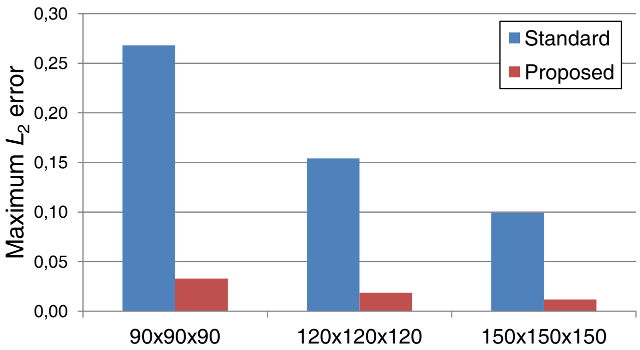

(a)

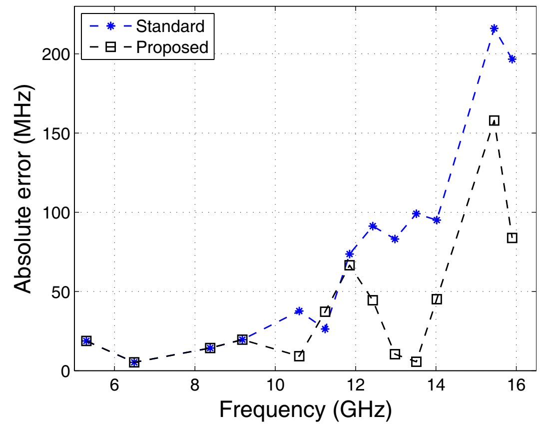

(b)

Figure 4: (a) Performance of the first scheme in a cubic cavity problem. (b) Performance of the second scheme in the detection of the cavity's resonant modes.

are consistent with the theoretical analysis and verify the superiority of the proposed approach, since an accuracy amendment by more than eight times is reported. Continuing with the same resonant structure, the wideband scheme of Subsection 2.2 is examined next, in the problem of detecting the resonant frequencies of the cavity's lowest 13 modes. Fig. 4(b) describes the absolute errors in the case of the fourth-order and the novel operators (13). It is concluded that this second modification provides a more precise discrete model than the standard solution, enabling more accurate predictions for the resonant frequencies (in average, the pertinent error is almost halved).

4. CONCLUSIONS

We have shown that performance enhancement of the ADI-FDTD method is feasible in two different ways. By combining the concept of artificial anisotropy with optimized spatial operators, precision is improved in the vicinity of a pre-selected wavelength. A more broadband correction is succeeded, if the dispersion relation is treated as an error formula, and a matching-terms procedure is applied. In both cases, considerable improvement compared to the standard fourth-order approximations has been verified, without any penalties regarding the computational overhead.

ACKNOWLEDGMENT

This work has been co-financed by the European Union and Greek funds via NSRF — Research Funding Program: Aristeia.

REFERENCES

1. Taflove, A. and S. C. Hagness, *Computational Electrodynamics: The Finite-Difference Time-Domain Method*, 3rd Edition, Artech House, Norwood, MA, 2005.
2. Namiki, T., "3-D ADI-FDTD method — Unconditionally stable time-domain algorithm for solving full vector Maxwell's equations," *IEEE Trans. Microw. Theory Techn.*, Vol. 48, No. 10, 1743–1748, Oct. 2000.
3. Tan, E. L., "Unconditionally stable LOD-FDTD method for 3-D Maxwell's equations," *IEEE Microw. Wireless Compon. Lett.*, Vol. 17, No. 2, 85–87, Feb. 2007.
4. Yang, Y., R. S. Chen, and E. K. N. Yung, "The unconditionally stable Cranc-Nicolson FDTD method for three-dimensional Maxwell's equations," *Microw. Opt. Technol. Lett.*, Vol. 48, No. 8, 1619–1622, Aug. 2006.
5. Grande, A., J. A. Pereda, A. Serroukh, I. Barba, A. C. Cabeceira, and J. Represa, "Reinterpreting four-stage split-step FDTD methods as two-stage methods," *IEEE Trans. Antennas Propag.*, Vol. 61, No. 11, 5818–5821, Nov. 2013.
6. Wang, M., Z. Wang, and J. Chen, "A parameter optimized ADI-FDTD method," *IEEE Antennas Wireless Propag. Lett.*, Vol. 2, 118–121, 2003.
7. Fu, W. and E. L. Tan, "A parameter optimized ADI-FDTD method based on the (2, 4) stencil," *IEEE Trans. Antennas Propag.*, Vol. 54, No. 6, 1836–1842, Jun. 2006.

8. Ahmed, I. and Z. Chen, " Error reduced ADI-FDTD methods," *IEEE Antennas Wireless Propag. Lett.*, Vol. 4, 323–325, 2005.
9. Fu, W. and E. L. Tan, "A compact higher-order ADI-FDTD method," *Microw. Opt. Technol. Lett.*, Vol. 44, No. 3, 273–275, Feb. 2005.
10. Zheng, H.-X. and K. W. Leung, "An efficient method to reduce the numerical dispersion in the ADI-FDTD," *IEEE Trans. Microw. Theory Tech.*, Vol. 53, No. 7, 2295–2301, Jul. 2005.
11. Zhang, Y., S.-W. Lu, and J. Zhang, "Reduction of numerical dispersion of 3-D higher order alternating-direction-implicit finite-difference time-domain method with artificial anisotropy," *IEEE Trans. Microw. Theory Tech.*, Vol. 57, No. 10. 2416–2428, Oct. 2009.
12. Kong, Y.-D., Q.-X. Chu, and R. Li, "Efficient unconditionally stable one-step leapfrog ADI-FDTD method with low numerical dispersion," *IET Microw., Antennas Propag.*, Vol. 8, No. 5, 337–345, 2014.